PCCP

www.rsc.org/pccp

PAPER

The origin of the enhanced oxygen storage capacity of $Ce_{1-x}(Pd/Pt)_xO_2$

David O. Scanlon,* Benjamin J. Morgan† and Graeme W. Watson*

Doping CeO_2 with Pd or Pt increases the oxygen storage capacity (OSC) and catalytic activity of this environmentally important material. To date, however, an understanding of the mechanism underlying this improvement has been lacking. We present a density functional theory analysis of Pd- and Pt-doped CeO_2, and demonstrate that the increased OSC is due to a large displacement of the dopant ions from the Ce lattice site. Pd(II)/Pt(II) (in a d^8 configuration) moves by ~ 1.2 Å to adopt a square-planar coordination due to crystal field effects. This leaves three three-coordinate oxygen atoms that are easier to remove, and which are the source of the increased OSC. These results highlight the importance of rationalizing the preferred coordination environments of both dopants and host cations when choosing suitable dopants for next generation catalysts.

Introduction

CeO_2 is one of the key materials in modern three-way catalysts, where it has been highly effective in the catalysis of automotive emissions, both as a support and as a catalyst itself.[1–3] This material also finds applications in other catalytic processes—*e.g.* water–gas shift reaction, and SO_x reduction—as well as being a component in gas sensors, intermediate temperature solid oxide fuel cells, and field-effect transistors.[4] The importance of ceria as a catalyst and a support stems from its oxygen storage capacity (OSC), which allows it to release oxygen under reducing conditions and to store oxygen by filling oxygen vacancies under oxidizing conditions.[5] Increasing the number and mobility of oxygen vacancies enhances the OSC and correspondingly improves catalytic activity.[6,7]

In this increasingly environmentally conscious age the search for improved catalysts has become inexorable. To this end, the doping of CeO_2 to produce next-generation catalysts has gathered much attention. In three-way catalysts noble metals normally sit atop the CeO_2 support. Recently, however, substitution of noble metals for Ce at lattice sites has been identified as a promising route to improved catalysts, and has been termed "noble metal ionic catalysis".[8]

$Ce_{1-x}NM_xO_{2-\gamma}$ solid solutions (x = 0.01–0.02), with NM = Cu^{II}, Pd^{II}, Pt^{II}, and Rh^{III}, have all been previously considered.[9–12] The presence of Pd in the lattice of ceria has been shown to have a beneficial catalytic effect for methane combustion,[13] and allows higher rates of NO and N_2O reduction,[14] and higher rates and lower activation energies for the oxidation of CO and hydrocarbons.[9,14] Pt-doped CeO_2 has demonstrated enhanced catalytic activity towards CO oxidation, hydrocarbon oxidation, and hydrogen adsorption, compared to that of Pt metal over CeO_2.[15] Pt-doped CeO_2 was also reported to catalyze the gas-phase hydrogenation of benzene to cyclohexane, yielding a turnover frequency an order of magnitude higher than for Pt metal, Pt/α-Al_2O_3, or Pt/γ-Al_2O_3.[16] The presence of these lower valence dopant ions results in the formation of charge-compensating oxygen vacancies neighbouring the dopant, which are observed in extended X-ray absorption fine structure (EXAFS) experiments.[9,17,18] For Pd and Pt, doping is formally described as

$$NM_{(s)} + Ce_{Ce}^{\times} + O_O^{\times} \rightarrow NM''_{Ce} + V_O^{\bullet\bullet} + Ce_{(s)}. \quad (1)$$

It should be emphasised that the vacancy formation that accompanies the substitution of Ce^{IV} with NM^{II} is not a reduction that contributes to the OSC, but is a consequence of the system maintaining charge neutrality as part of the doping process.

Hermansson and co-workers have previously used the local density approximation (LDA) + U approach to model the doping of CeO_2 with Pd and Pt,[19,20] with the formation of the charge-compensating vacancy incorrectly considered as the reduction energy. The authors reported that the replacement of a Ce^{IV} in both cases resulted in a very small relaxation around the dopants.[19,20] Subsequent removal of an oxygen neighbouring the dopant yielded "reduction" energies of 57 kJ mol^{-1} and 93 kJ mol^{-1} for Pd-doped and Pt-doped ceria, respectively. These results would suggest that the removal of an oxygen next to the dopant during formation of a charge-compensating vacancy *costs* energy.[19,20] This is at variance with previous X-ray photoelectron spectroscopy studies that indicate Pd and Pt to be present preferentially in

School of Chemistry, Trinity College Dublin, Dublin 2, Ireland.
E-mail: scanloda@tcd.ie, watsong@tcd.ie
† Current address: Department of Materials, University of Oxford, Parks Road, OX1 3PH, UK.
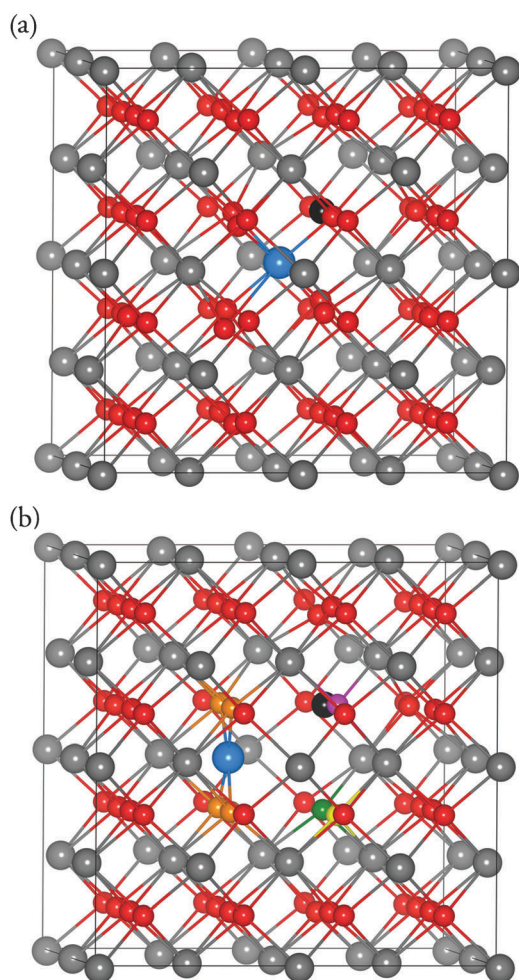
Fig. 1 (a) Pd/Pt dopant in CeO$_2$ sitting on the perfect Ce lattice position. (b) Pd/Pt sitting in a square planar coordination between four lattice oxygen. Blue spheres denote the Pd/Pt dopant, grey and red spheres denote the Ce and O ions respectively. The black spheres represent the position of the charge-compensating vacancy, and the pink, yellow and green spheres represent the under-coordinated oxygen ions O$_a$, O$_b$, O$_c$ respectively.

the $+2$ oxidation state, and accompanied by spontaneously formed charge-compensating vacancies.[9,18]

Despite the reported improvements in catalytic activity and OSC, the underlying reason for these has remained unclear. In this article we study the effect of Pd and Pt substitution in CeO$_2$, focusing on the oxidation state and geometry of the dopants, and their effect on oxygen vacancy formation. Using the insights gained from this analysis, we propose guidelines for the rational design of next generation catalysts.

I. Theoretical methods

All calculations were performed using the VASP package,[21,22] in which the valence electronic states are expanded within a plane-wave basis. The valence–core interaction is described using the projector augmented wave (PAW) approach,[23] and cores of [He] for oxygen, and [Xe] for cerium are used. The Perdew–Burke–Ernzerhof generalized gradient approximation (GGA) exchange–correlation functional was used,[24] and

supplemented by a Dudarev$+U$ term.[25] Standard density functional calculations are unable to correctly describe the electronic structure of reduced CeO$_2$,[26,27] due to the self-interaction error inherent to such functionals, and which is acute for strongly localised orbitals such as transition metal d or rare earth f states.[28–30] The inclusion of a $+U$ correction allows this deficiency to be addressed without an excessive increase in the computational cost of the calculations. The sensitivity of results to the value of U for GGA$+U$ calculations of ceria have previously been described,[26,27] with a value of $U = 5$ eV selected for the Ce f orbitals. The suitability of this value of U has subsequently been verified by other studies,[31,32] and has been used many times to successfully model reduced CeO$_2$ systems.[33–36] GGA$+U$ has yielded results in excellent quantitative agreement with hybrid DFT approaches.[37–40] No $+U$ term was applied to the dopant states, as the $+U$ is used in this case as an energetic penalty to partial occupation, meaning that localized behaviour is favoured over delocalized behaviour. As there is only one dopant in the supercell, if charge wished to localize on the dopant, there will be no delocalization issue. A cutoff of 500 eV was used for the all calculations, with the Brillouin zone sampled using a $4 \times 4 \times 4$ Monkhorst–Pack grid for the bulk and a $2 \times 2 \times 2$ sampling for the 96 atom supercell. All calculations were spin polarized and were deemed to have converged when the forces on all the atoms were less than 0.01 eV Å^{-1}.

II. Results

CeO$_2$ is a wide band gap insulator that adopts a cubic fluorite structure with a lattice parameter, a, of 5.41. The calculated lattice parameter of CeO$_2$ is $\sim$5.49 Å at the GGA$+U$; $U = 5$ eV level, which is within 1.5% of experiment. Using a $2 \times 2 \times 2$ (96 atom) supercell, we have calculated the formation energy of an oxygen vacancy in pure CeO$_2$ to be 253 kJ mol^{-1}, which is consistent with previous theoretical studies.[41]

For the incorporation of Pd/Pt into the CeO$_2$ lattice we first considered the case of single Pd/Pt substituting for a Ce^{IV} within the 96 atom cell, with subsequent charge-compensating vacancy formation. This was done in two ways: (i) similar to the calculations of Hermansson and co-workers, we replaced one Ce^{IV} with a Pd/Pt on the perfect lattice site, and allow this to relax fully, followed by the subsequent removal of an oxygen neighbouring the dopant (charge-compensating vacancy formation, Fig. 1(a)) and (ii) the Pd/Pt is displaced off the perfect Ce lattice site upon charge-compensating vacancy formation, to test for lower energy distorted configurations.

From method (i), the energy to form a charge-compensating vacancy in Pd/Pt doped CeO$_2$ was found to be 64 kJ mol^{-1} and 115 kJ mol^{-1} for Pd and Pt, respectively, which is in reasonable agreement with the previous LDA$+U$ results of Hermansson and co-workers.[19,20] From method (ii), however, once the Pd/Pt is allowed to move off the perfect Ce lattice site, it undergoes a large lattice distortion away from the charge-compensating vacancy site to assume a *square planar* coordination between four lattice oxygens, Fig. 1(b). The charge-compensating vacancy formation energies in this case

are now -69 kJ mol^{-1} and -72 kJ mol^{-1} for Pd and Pt, respectively.

The large lattice distortion lowers the energy of the square planar configuration compared to the distorted cubic configuration proposed previously[19,20] by 134 kJ mol^{-1} and 186 kJ mol^{-1} for Pd and Pt, respectively. Indeed, with a charge-compensating vacancy present, Pd/Pt will have an oxidation state of $+2$ with a d^8 configuration, which is *not* known to adopt the cubic coordination of the perfect Ce lattice position.[42] Our results indicates that the NM^{IV} to NM^{II} plus charge-compensating vacancy transition is in fact spontaneous, which is consistent with experiment, with a charge-compensating vacancy expected to be neighbouring the dopant.[9,17,18] The failure to account for the large lattice distortion explains why Hermansson and co-workers predicted the incorporation of the noble metal at a higher oxidation state, and the formation of the charge-compensating vacancy to be a reduction. It is also instructive to note that, in supercell defect calculations, breaking of the symmetry has been shown to be vital to obtain quantitatively accurate defect geometries.[43,44]

The large lattice distortion places the Pd/Pt in a square planar coordination environment between 4 lattice oxygens, and leaves three *under-coordinated* oxygen atoms, Fig. 1(b). Table 1 lists calculated formation energies for vacancies at each of the three under-coordinated oxygen. The oxygen vacancy formation energy decreases from 253 kJ mol^{-1} in pure CeO$_2$ to 173 kJ mol^{-1} for Pd-doped and 170 kJ mol^{-1} for Pt-doped CeO$_2$. For all three under-coordinated oxygen atoms, the energy to form an oxygen vacancy is *significantly* lowered compared to pure CeO$_2$. For both dopants, the under-coordinated oxygen that is furthest from the charge-compensating vacancy (denoted O$_b$, yellow sphere in Fig. 1(b)), is the easiest to remove, as this minimizes the repulsion between the two positively charged vacancies. The other under-coordinated oxygen ions (O$_a$ and O$_c$) have a higher vacancy formation energy, but are still easier to remove than an oxygen from pure CeO$_2$.

The excess electrons left behind upon vacancy formation localize on two Ce ions neighbouring the vacancy, formally reducing them to Ce^{III}, as illustrated in Fig. 2. The lowering of the oxygen vacancy formation energy in the doped supercell compared to the pure supercell indicates that the large lattice distortion serves to weaken the bonds around the under-coordinated oxygen, making it easier to remove them. In the work of Hermansson and co-workers, the Pd/Pt states in the band gap are proposed as the origin of the enhanced reducibility.[19,20] As their study does not find the lowest energy square planar configuration, and ignores the formation of a charge compensating vacancy, the author's calculated PEDOS for doped CeO$_2$ shows Pd/Pd defect states in the band gap, with

Table 1 GGA $+ U$ calculated oxygen vacancy formation energies for the three under-coordinated oxygens in Pd/Pt doped CeO$_2$ supercell, O$_a$, O$_b$, O$_c$. All energies are quoted in kJ mol^{-1}

	V_{O_a}	V_{O_b}	V_{O_c}
CeO$_2$:Pd	224	173	228
CeO$_2$:Pt	207	170	218

some unoccupied defect states in the spin down (Beta spin).[19,20] Subsequent oxygen vacancy formation fills these unoccupied states, leaving the non-spin paired Pd/Pt states in the band gap.[19,20]

In our study, we have uncovered the ground state structure of Pd/Pt doped CeO$_2$, which is in the square planar coordination with a charge compensating vacancy neighbouring the dopant. In a square planar d^8 configuration, the electrons spin pair, as can be seen in our calculated PEDOS for Pd doped CeO$_2$, Fig. 3(a). Upon reduction of the system (removal of an oxygen vacancy), the excess electrons localize on the two neighbouring Ce atoms. This is clearly shown in the PEDOS of the reduced Pd doped supercell, Fig. 3(b). Therefore, our study shows that the large lattice distortion and the reducibility of Ce^{IV} to Ce^{III} are the key factors in the lower reduction energy of Pd/Pt doped CeO$_2$.

Ligand field theory predicts that a d^8 ion will prefer a square planar coordination over that of a cubic coordination. Within a cubic crystal field the d^8 cation will have two paired electrons and two unpaired electrons in three high energy t_{2g} orbitals, Fig. 4. This degeneracy can be lifted by adopting a square planar arrangement, and the now doubly occupied d_{xy} and d_{z^2} orbitals are lowered in energy, stabilizing the ion, Fig. 4.[42] It is interesting to consider whether this crystal field preference for square planar coordination for the d^8 dopants is sufficient to induce the large lattice distortion, or whether the charge-compensating vacancy formation that accompanies such doping is necessary. To address this we have simulated the effect of a single N^{II} in the 96 atom cell with no vacancy present by adding two electrons to the system. We tested the stability and spin state of two configurations: (i) Pd^{II}/Pt^{II} on the perfect *cubic* Ce lattice site, and (ii) Pd^{II}/Pt^{II} in square planar arrangement between four lattice oxygens. The square planar configuration was 133 kJ mol^{-1} and 238 kJ mol^{-1}, more stable than the cubic for Pd and Pt, respectively. It is clear that even in the absence of a charge-compensating vacancy, Pd^{II} and Pt^{II} both strongly favour square planar coordination. The well known preference for these metals to adopt square planar coordination[42] is sufficient to drive the large lattice distortion in doped CeO$_2$.

III. Discussion

Noble metal ionic catalysis has emerged over the past decade as a viable alternative to the well established metal oxide catalysts.[45–47] Despite multiple reports of improved catalytic behaviour of these noble-metal-doped oxides over pure oxide systems and even over metals supported on metal oxides, little is actually known about the true effect of these noble metal dopants on reducibility and catalytic selectivity/activity. To aid in progressing the development of noble metal ionic catalysis it is vital that a nanoscopic understanding of the fundamental role of the dopant in the host oxide is elucidated.

Our calculations have revealed that the driving force for enhanced reducibility in Pd/Pt doped CeO$_2$ is the preference for square planar coordination displayed by d^8 Pd^{II}/Pt^{II}. Both Pt and Pd prefer to be incorporated into the CeO$_2$ lattice as Pd^{II}/Pt^{II}, with an associated *charge-compensating* oxygen vacancy, and not as d^6 Pd^{IV}/Pt^{IV}. The driving force for the
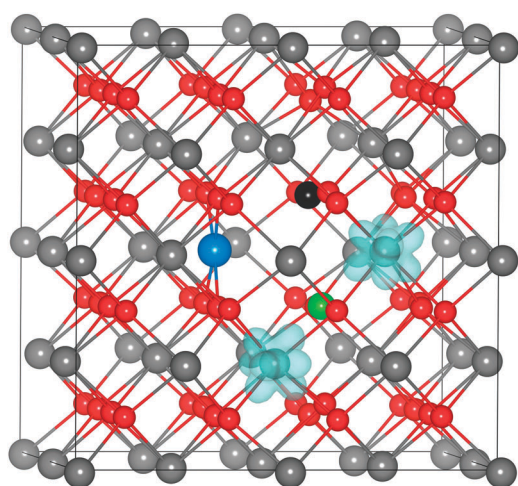
Fig. 2 Geometry and spin density of Pt-doped CeO_2, with a vacancy in the O_b position. The blue, grey, red, black, and green spheres represent the Pt, Ce, O, charge compensating vacancy, and "reduction" vacancy respectively. The light blue spin density isosurface is shown at 0.05 e Å^{-3}.
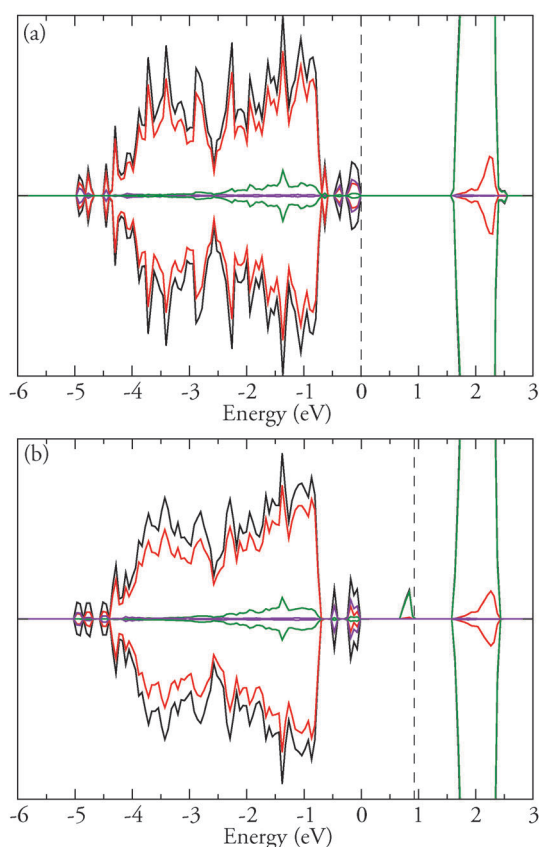

Fig. 3 Atom projected electronic densities of states for (a) Pd doped CeO_2 with a charge compensating vacancy, and (b) reduced Pd doped CeO_2 with a charge compensating vacancy. O p states are red, Ce f states are green and Pd d states are violet. The top of the valence band is aligned to 0 eV with the vertical dashed line showing the position of the highest occupied state.

large lattice distortion is the strong preference of Pd^{II}/Pt^{II} to obtain square planar coordination environments. This large
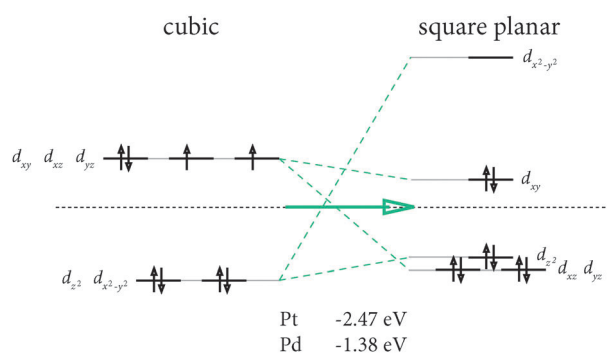

Fig. 4 Crystal field splitting of a d^8 ion in a cubic (left) and square planar (right) field, with the associated stabilization energies.

lattice distortion is determined by the electronic configuration of the noble metal dopant, and not purely by the valence of the dopant. To test this hypothesis, we carried out test calculations of Zn doped CeO_2, finding that d^{10} Zn^{II} ions do not wish to adopt square planar coordination, or to remain on the cubic Ce lattice site, but rather prefer to distort to form 4 short and 4 long Zn–O bonds. It is not surprising that Zn does not take up a square planar configuration as Zn prefers a tetrahedral coordination, as seen in ZnO.[48] The electronic configuration and size of a dopant is thus of vital importance to the type of distortion that can be induced in the host oxide.

Normally, when one considers a suitable dopant to enhance the reducibility of a material, the main focus is placed on the ionic radius of the dopant, in an effort to distort the coordination of a lattice oxygen and weaken some of the M–O bonds.[49–51] It is generally accepted that, for example, the increase in OSC of Zr and Ti doped CeO_2 can be explained by the weakening of oxygen bonds around the dopant ion,[50,51] with a recent study highlighting the role of relaxation around the dopant in Zr doped CeO_2.[52] Our calculations indicate that another significant factor is the preferred coordination environment of the dopant, especially in the case of d block transition metals. Careful choice of a dopant with a suitably small ionic radius, and a *significant* difference in preferred coordination environment compared to the host cation, will lead to maximum effect on the oxygen bonding. These considerations suggest it is advantageous to choose a dopant with a normal coordination environment in its own native oxide that is lower than the coordination number in the host oxide, to maximize the distortion, and yield a reduced coordination around some of the oxygen ions. Hence, a careful consideration of the coordination "requirements" of the dopant in the host oxide could be exploited in the prediction in developing new improved metal oxide catalysts. It is therefore likely that other d^8 dopants, such as Ni^{II}, or even a d^9 dopant, such as Cu^{II}, would be excellent dopants to test these criteria.

The consequences of these electronic structure driven distortions extend beyond the OSC of CeO_2. In the field of dilute magnetic semiconductors (DMS), doping of oxide semiconductors with magnetic cations to induce ferromagnetism is of huge interest.[48] In some cases, *e.g.* ZnO:Co, the coordination environments of the dopant (tetrahedral Co^{II} in Co_3O_4) and host cation (tetrahedral Zn^{II} in ZnO) match and are not an issue,[48] however, in other cases the coordination of the ion will

4282 | *Phys. Chem. Chem. Phys.*, 2011, **13**, 4279–4284

This journal is © the Owner Societies 2011

have a large impact on the splitting of the d levels. A good example of this is CeO_2 : Co, which has been reported to show room temperature ferromagnetism.[53,54] This has yet to be satisfactorily explained using first principles, and to date, *all* first principles calculations have assumed the Co to sit on the perfect Ce lattice cite.[55,56] It would appear unlikely, based on our current analysis for Pd/Pt, that a d^7 (Co[II]) or a d^6 (Co[III]) ion would prefer to sit on a perfect lattice site.

IV. Conclusion

The origin of the improved OSC of Pd/Pt-doped CeO_2 has been shown to be a consequence of the crystal field stabilization of the d^8 dopant ions in a square planar coordination environment. This requires the dopant Pd[II]/Pt[II] to undergo a large lattice distortion away from the perfect Ce[IV] lattice site to assume a square planar coordination with four lattice oxygens. This large lattice distortion leaves three oxygen atoms under-coordinated in the vicinity of the dopant, making their removal under reducing conditions much more facile. These findings highlight the importance of the preferred coordination environment of the dopant compared with the cation coordination of the host oxide. We propose that when designing next-generation oxide catalysts with increased OSC, it is advantageous to select dopants based on an understanding of oxidation state, ionic radius, and additionally electronic structure and corresponding preferred coordination environments.

Acknowledgements

References

1 A. Trovarelli, *Catalysis by Ceria and Related Materials*, Imperial College Press, UK, 2002.
2 D. O. Scanlon, N. M. Galea, B. J. Morgan and G. W. Watson, *J. Phys. Chem. C*, 2009, **113**, 11095–11103.
3 S. Fabris, S. de Gironcoli, S. Baroni, G. Vicario and B. Gabriele, *Phys. Rev. B: Condens. Matter Mater. Phys.*, 2005, **71**, 041102(R).
4 C. Loschen, A. Migani, S. T. Bromley, F. Illas and K. M. Neyman, *Phys. Chem. Chem. Phys.*, 2008, **10**, 5730–5738.
5 A. Trovarelli, *Comments Inorg. Chem.*, 1999, **20**, 263–284.
6 M. Daturi, N. Bion, J. Saussey, J.-C. Lavalley, C. Hedouin, T. Seguelong and G. Blanchard, *Phys. Chem. Chem. Phys.*, 2001, **3**, 252–255.
7 N. V. Skorodumova, S. I. Simak, B. I. Lundqvist, I. A. Abrikosov and B. Johansson, *Phys. Rev. Lett.*, 2002, **89**, 166601.
8 M. S. Hegde, G. Madras and K. C. Patil, *Acc. Chem. Res.*, 2009, **42**, 704–712.
9 K. R. Priolkar, P. Bera, P. R. Sarode, M. Hegde, S. Emura, R. Kamashiro and N. P. Lalla, *Chem. Mater.*, 2002, **14**, 2120–2128.
10 P. Bera, K. R. Priolkar, P. R. Sarode, M. S. Hegde, S. Emura, R. Kumashiro, V. Jayaram and N. P. Lalla, *Chem. Mater.*, 2002, **14**, 3591–3601.
11 P. Bera, K. R. Priolkar, A. Gayen, P. R. Sarode, M. S. Hegde, S. Emura, R. Kumashiro, V. Jayaram and G. N. Subbanna, *Chem. Mater.*, 2003, **15**, 2049–2060.
12 A. Gayen, K. R. Priolkar, P. R. Sarode, V. Jayaram, M. S. Hegde, V. Jayaram and S. Emura, *Chem. Mater.*, 2004, **16**, 2317.
13 A. Primavera, A. Trovarelli, C. de Leitenburg, G. Dolcetti and J. Llorca, *Stud. Surf. Sci. Catal.*, 1998, **119**, 87–92.
14 S. Roy, A. Marimuthu, M. S. Hegde and G. Madras, *Appl. Catal., B*, 2007, **71**, 23–31.
15 T. Baidya, A. Gayen, M. S. Hegde, N. Ravishankar and D. L, *J. Phys. Chem. B*, 2006, **110**, 5262–5272.
16 K. Nagaveni, G. Sivalingam, A. Gayen, A. Madras and M. S. Hegde, *Catal. Lett.*, 2003, **88**, 73–81.
17 P. Bera, A. Gayen, M. S. Hegde, N. P. Lalla, L. Spadero, F. Frusteri and F. J. Arena, *J. Phys. Chem. B*, 2003, **107**, 6122–6130.
18 A. Gayen, T. Baidya, A. S. Prakash, N. Ravishankar and M. S. Hegde, *Indian J. Chem. A*, 2005, **44A**, 34–48.
19 Z. Yang, G. Luo, Z. Lu and K. Hermansson, *J. Chem. Phys.*, 2007, **127**, 074704.
20 Z. Yang, G. Lu, Z. Lu, T. K. Woo and K. Hermansson, *J. Phys.: Condens. Matter*, 2008, **20**, 035210.
21 G. Kresse and J. Hafner, *Phys. Rev. B: Condens. Matter*, 1994, **49**, 14251–14271.
22 G. Kresse and J. Furthmuller, *Comput. Mater. Sci.*, 1996, **6**, 15–50.
23 P. E. Blöchl, *Phys. Rev. B: Condens. Matter*, 1994, **50**, 17953.
24 J. P. Perdew, K. Burke and M. Ernzerhof, *Phys. Rev. Lett.*, 1996, **77**, 3865.
25 S. L. Dudarev, G. A. Botton, S. Y. Savrasov, C. J. Humphreys and A. P. Sutton, *Phys. Rev. B: Condens. Matter Mater. Phys.*, 1998, **57**, 1505.
26 M. Nolan, S. Grigoleit, D. C. Sayle, S. C. Parker and G. W. Watson, *Surf. Sci.*, 2005, **576**, 217–229.
27 M. Nolan, S. C. Parker and G. W. Watson, *Surf. Sci.*, 2005, **595**(1–3), 223–232.
28 B. J. Morgan and G. W. Watson, *Surf. Sci.*, 2007, **601**, 5034–5041.
29 D. O. Scanlon, A. Walsh, B. J. Morgan and G. W. Watson, *J. Phys. Chem. C*, 2008, **112**, 9903–9911.
30 B. J. Morgan, D. O. Scanlon and G. W. Watson, *J. Mater. Chem.*, 2009, **19**, 5175–5178.
31 D. A. Andersson, S. I. Simak, B. Johansson, I. A. Abrikosov and N. V. Skorodumova, *Phys. Rev. B: Condens. Matter Mater. Phys.*, 2007, **75**, 035109.
32 C. Zhang, A. Michaelides, D. A. King and S. J. Jenkins, *Phys. Rev. B: Condens. Matter Mater. Phys.*, 2009, **79**, 075433.
33 M. Nolan, S. C. Parker and G. W. Watson, *Phys. Chem. Chem. Phys.*, 2006, **8**, 216.
34 M. Nolan and G. W. Watson, *J. Phys. Chem. B*, 2006, **110**, 16600–16606.
35 M. Nolan, S. C. Parker and G. W. Watson, *J. Phys. Chem. B*, 2006, **110**, 2256.
36 N. M. Galea, D. O. Scanlon, B. J. Morgan and G. W. Watson, *Mol. Simul.*, 2009, **35**, 577–583.
37 M. V. Ganduglia-Piravano, J. L. F. Da Silva and J. Sauer, *Phys. Rev. Lett.*, 2009, **102**, 026101.
38 H. Y. Li, H. F. Wang, Z. Q. Gong, Y. L. Guo, Y. Giuo, G. Lu and P. Hu, *Phys. Rev. B: Condens. Matter Mater. Phys.*, 2009, **79**, 193401.
39 J. L. F. Da Silva, M. V. Ganduglia-Pirovano, J. Sauer, V. Bayer and G. Kresse, *Phys. Rev. B: Condens. Matter Mater. Phys.*, 2007, **75**, 045121.
40 C. Loschen, J. Carrasco, K. M. Neyman and F. Illas, *Phys. Rev. B: Condens. Matter Mater. Phys.*, 2007, **75**, 035115.
41 P. R. L. Keating, D. O. Scanlon and G. W. Watson, *J. Phys.: Condens. Matter*, 2009, **21**, 405502.
42 J. R. Gispert, *Coordination Chemistry*, Wiley-VCH Verlag GmbH & Co. KGaA, Weinheim, Germany, 2008.
43 D. O. Scanlon, A. Walsh, B. J. Morgan, M. Nolan, J. Fearon and G. W. Watson, *J. Phys. Chem. C*, 2007, **111**(22), 7971–7979.
44 A. A. Sokol, A. Walsh and C. R. A. Catlow, *Chem. Phys. Lett.*, 2010, **492**, 44–48.
45 S. Roy, A. Marimuthu, M. S. Hegde and G. Madras, *Appl. Catal., B*, 2007, **73**, 300–310.
46 S. Roy and M. S. Hegde, *Catal. Commun.*, 2008, **9**, 811–815.
47 S. Roy, M. S. Hegde and G. Madras, *Appl. Energy*, 2009, **86**, 2283–2297.
48 A. Walsh, J. L. F. Da Silva and S. H. Wei, *Phys. Rev. Lett.*, 2008, **100**, 256401.

This journal is © the Owner Societies 2011

Phys. Chem. Chem. Phys., 2011, **13**, 4279–4284 | 4283

49 V. Butler, C. R. A. Catlow, B. E. F. Fender and J. H. Harding, *Solid State Ionics*, 1983, **8**, 109–103.

50 G. Dutta, U. V. Waghmare, T. Baidya, M. S. Hegde, K. R. Priolkar and P. R. Sarode, *Chem. Mater.*, 2006, **18**, 3249.

51 G. Dutta, U. V. Waghmare, T. Baidya, M. S. Hegde, K. R. Priolkar and P. R. Sarode, *Catal. Lett.*, 2006, **108**, 165–172.

52 H. F. Wang, X. Q. Gong, Y. L. Guo, Y. Guo, G. Z. Lu and P. Hu, *J. Phys. Chem. C*, 2009, **113**, 10229–10232.

53 Q. W. Wen, H. W. Zhang, Y. W. Song, Q. H. Yang, H. Zhu and J. Q. Xiao, *J. Phys.: Condens. Matter*, 2007, **19**, 246205.

54 Y. Q. Song, H. W. Zhang, Q. Y. Wen, L. Peng and J. Q. Xiao, *J. Phys.: Condens. Matter*, 2008, **20**, 255210.

55 Y. Q. Song, H. W. Zhang, Q. H. Yang, Y. L. Liu, Y. X. Li, L. R. Shah, H. Zhu and J. Q. Xiao, *J. Phys.: Condens. Matter*, 2009, **21**, 125504.

56 V. Ferrari, A. M. Llois and V. Lidosola, *J. Phys.: Condens. Matter*, 2010, **22**, 276002.